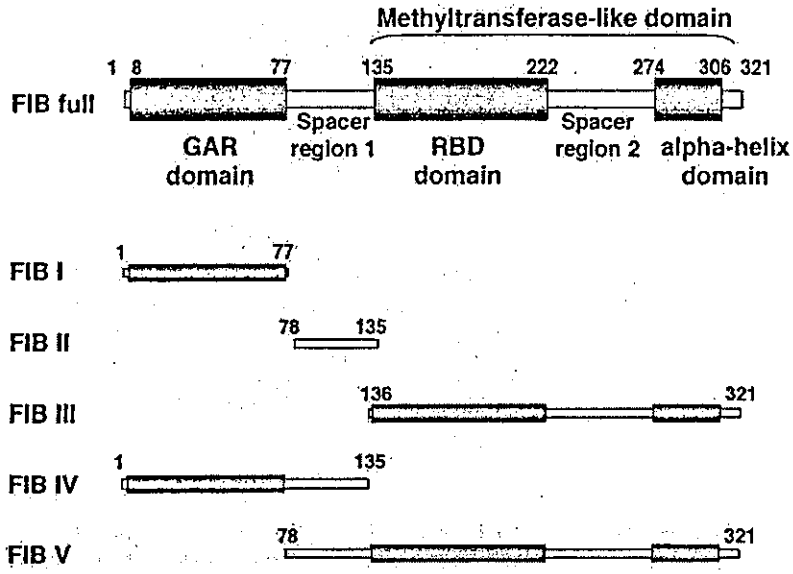

FIG. 1. **Schematic representation of domain structures of FIB and truncation mutants.** Full-length FIB and truncation mutants are shown. The N-terminal glycine- and arginine-rich (*GAR*) domain, RNA-binding domain (*RBD*), and α-helix domain are *shaded in gray*, and the spacer regions 1 and 2 are indicated. The methyltransferase-like domain is composed of the RBD, spacer region 2, and α-helix domain. The residue numbers of FIB and the truncation mutants are indicated above each diagram. A FLAG tag (not shown) was added to the N terminus of each peptide. For FIB truncation mutants, the SV40 antigen nuclear localization signal and the HIV Rex nucleolar localization signal were added between the FLAG tag and the N terminus of each mutant (not shown in the figure).

of FIB with both SMN protein and the DEAD box RNA helicase p68 (19, 21). A centrally located 90-residue sequence resembles an RNA-binding domain (RBD) present in various snRNPs. This RBD together with the C-terminal α-helix domain and the intervening spacer (spacer region 2) constitutes a methyltransferase-like domain that contains an *S*-adenosyl methionine-binding motif (14, 22). Replacement of two residues in the Nop1p *S*-adenosyl methionine-binding motif results in temperature sensitivity and a drastic reduction in nascent rRNA transcript methylation under restrictive conditions (18). Thus, the methyltransferase-like domain is responsible for FIB methyltransferase activity. The C-terminal α-helix domain is composed of ~30 residues, and although this domain probably targets FIB to Cajal bodies, spacer region 2 appears to target FIB to the fibrillar regions. However, the targeting of FIB in both instances occurs only in the presence of the RBD (3). Although it is well established that FIB plays a role in ribosome biogenesis within the nucleolus, its role in Cajal bodies is not understood.

Our recent studies have used proteomic methodology to characterize a series of preribosomal ribonucleoprotein (pre-rRNP) complexes formed in mammalian cells. We have thus far isolated and analyzed the pre-rRNP complexes associated with human nucleolin (25), parvulin (26), and Nop56p (27). These studies demonstrate the applicability of proteomic analysis to the study of human ribosome biogenesis and have identified a number of mammalian counterparts of yeast trans-acting factors involved in this process. Furthermore, several candidate mammalian trans-acting factors were identified that were not previously identified in yeast. Here, we present a proteomic analysis of FIB-associated protein complexes. In addition to the association of FIB with pre-rRNP complexes, we found that this protein interacts with a sub-complex containing a minimal set of proteins including SF2A-p32, PRMT5, tubulin α3, tubulin β1, and PRMT1. The FIB GAR domain and the spacer region 1 interact directly with SF2A-p32, whereas the methyltransferase-like domain interacts with PRMT5. These results provide new clues to the precise functions of FIB not only in ribosome biogenesis but also in sn(o)RNP biogenesis and mRNA processing in Cajal bodies.

EXPERIMENTAL PROCEDURES

Materials—Human kidney cell line 293EBNA, Opti-MEM, and LipofectAMINE were purchased from Invitrogen (Grand Island, NY). Dulbecco's modified Eagle's medium, anti-FLAG M2 affinity gel, FLAG peptide, IGEPAL CA630, RNase A, and α-cyano-4-hydroxycinnamic acid were from Sigma-Aldrich Chemical (Steinheim, Germany). Alkaline phosphatase-conjugated anti-mouse IgG was from Amersham Biosciences (Uppsala, Sweden). Alexa Fluor 488-conjugated rabbit anti-mouse IgG antibody was from Molecular Probes, Inc. (Eugene, OR). Trypsin (sequence grade) was from Promega (Madison, WI) and *Achromobacter lyticus* protease I (Lys-C) was from WAKO Pure Chemicals (Osaka, Japan). ZipTipC18 was from Millipore (Billerica, MA). LA*Taq* DNA polymerase was from Takara (Shiga, Japan). Protease inhibitor mixture Complete Mini was from Roche Diagnostics (Mannheim, Germany). Collagen I-coated Biocoat 8-well culture slides were from BD Biosciences (Franklin Lakes, NJ). All other reagents were from WAKO Pure Chemicals.

Vectors for Epitope-tagged FIB and FIB Truncation Mutants and Expression in 293EBNA Cells—The FIB expression plasmid was constructed using a PCR-amplified DNA fragment comprising the FIB open reading frame with the FLAG tag at its N terminus (Fig. 1). This fragment was introduced between the NheI and the BamHI sites of the mammalian expression vector, pcDNA3.1 (+) (Invitrogen). The PCR primer set was 5′-ATATATCTAGAGCCACCATGGACTACAAGGACGACGACGACAAGAAGCCAGGATTCAGTCCCCGT-3′ and 5′-TATAGGATCCTCAGTTCTTCACCTTGGGGGG-3′, and human placenta cDNA (OriGene Technologies, Inc., Rockville, MD) was used as the template.

The DNA fragment encoding the FLAG tag along with the nucleolar localization signal (NLS) of HIV Rex (TRRRPRRSQRKR) (28) and the SV40 nuclear localization signal (NS) (PKKKRKV) (29) was synthesized by PCR using the oligonucleotide sets 5′-TATAGCTAGCGCCACCATGGACTACAAGGACGACGACGACAAGACCCGTCGGAGGCCCCG-3′ and 5′-TCTTTTTCTTTGGGATCGGCGGGGCCTCCGACGGGT-3′, and 5′-GATCCCAAAGAAAAAGAGCCAGCCCAAAAAAGAAGAGAAA-3′ and 5′-ATATAGGATCCTACCTTTCTCTTCTTTTTTGG-3′. The amplified fragment was subcloned between the NheI and the BamHI sites of pcDNA3.1(+), and the resulting plasmid was designated pcDNA3.1-NLS. All the expression plasmids of the FIB deletion mutants were constructed by introducing PCR-amplified fragments between the BamHI and XhoI sites downstream of the FLAG tag/NLS/NS in pcDNA3.1-NLS. Primer sets used for the amplification of FIB deletion mutants were as follows; 5′-ATATAGGATCCAAGCCAGGATTCAGTCCCCGT-3′ and 5′-TATATCTCGAGTCATTTTCCTCCCCGACCACGACC-3′ for FIB I (residues 2–77), 5′-ATATAGGATCCAGAGGAAACCAGTCGGGGAAG-3′ and 5′-TATATCTCGAGTCATCGGTACTCAAATTTGTCATC-3′ for FIB II (residues 78–135), 5′-ATATAGGATCCGCCTGGAACCCCTTCCGCTCC-3′ and 5′-TATATCTCGAGTCAGTTCTTCACCTTGGGGGG-3′ for FIB III (residues 136–321), 5′-ATATAGGATCCAAGCCAGGATTCAGTCCCCGT-3′ and 5′-TATATCTCGAGTCATCGGTACTCAAATTTGTCATC-3′ for FIB IV (residues 2–135), 5′-ATATAGGATCCAGAGGAAACCAGTCGGGGAAG-3′ and 5′-TATATCTCGAGTCAGTTCTTCACCTTGGGGGG-3′ for FIB V (residues 78–321).

Human 293EBNA cells were cultured in Dulbecco's modified Eagle's medium supplemented with 10% heat-inactivated fetal calf serum, streptomycin (0.1 μg/ml), and penicillin G (100 units/ml) at 37 °C in an

incubator under 5% CO_2. Subconfluent cells in 90-mm dishes were transfected with 10 μg of expression plasmid DNA using LipofectAMINE, and the transfected cells were grown for 48 h at 37 °C.

Isolation of FIB- and Its Truncated Mutant-associated Complexes—At 48 h post-transfection, 293EBNA cells were harvested and washed with PBS and lysed in lysis buffer (50 mM Tris-HCl, pH 8.0, 150 mM NaCl, 0.5% IGEPAL CA630) containing a protease inhibitor mixture on ice for 30 min. The soluble fraction was obtained by centrifugation at 15,000 rpm for 30 min at 4 °C and was incubated with 20 μl of anti-FLAG M2-agarose beads for 4 h at 4 °C for immunoprecipitation of FIB-associated complexes or overnight at 4 °C for deletion mutant-associated complexes. After washing the agarose beads five times with lysis buffer and once with 50 mM Tris-HCl, pH 8.0, 150 mM NaCl, the complexes bound to the agarose beads were eluted with 20 μl of 50 mM Tris-HCl, pH 8.0, 150 mM NaCl containing 500 μg/ml FLAG peptide. The eluted complexes were analyzed by SDS-PAGE.

Ribonuclease Treatment of the FIB- and Truncation Mutant-associated Complexes—The immunoprecipitated FIB and truncation mutant-associated complexes described above were incubated with 50 mM Tris-HCl, pH 8.0, 150 mM NaCl containing 1 μg/ml RNase A for 10 min at 37 °C, washed twice with lysis buffer, and then once with 50 mM Tris-HCl, pH 8.0, 150 mM NaCl, and eluted with buffer containing the FLAG peptide as described above.

Immunocytochemistry—293EBNA cells were grown on Collagen I-coated 8-well culture slides and transfected with expression plasmids using LipofectAMINE. Prior to fixation, cells were washed with PBS followed by incubation with 3.7% formaldehyde in PBS. After several washes with PBS-T (PBS containing 0.05% (w/v) Tween 20), the cells were incubated with PBS containing 0.1% (w/v) Triton X-100 for 5 min at room temperature. The cells were then blocked by 3% (w/v) nonfat dried milk in PBS and were incubated with anti-FLAG for 1 h at room temperature. The cells were rinsed in PBS-T and then incubated with Alexa Fluor 488-conjugated anti-mouse IgG for 1 h at room temperature, followed by three washes with PBS-T. The resulting cells were examined with a confocal laser-scanning microscope TCS (Leica Microsystems AG, Wetzlar, Germany).

Protein Identification by the Peptide Mass Fingerprinting Method—Protein-containing SDS-PAGE gel fragments were subjected to in-gel digestion with trypsin as previously described (25). The resulting peptides were recovered and analyzed for peptide mass fingerprints using a PE Biosystems MALDI-TOF MS (Voyager DE-STR) as described previously (25). Peptide masses were searched with 50 ppm mass accuracy using the data base fitting program MS-Fit (available at prospector.ucsf.edu), and protein identification was performed according to the criteria described previously (25).

Protein Identification by LC-MS/MS Analysis—The FIB- and truncation mutant-associated complexes were digested with Lys-C, and the resulting peptides were analyzed using a nanoscale LC-MS/MS system as described (30). The peptide mixture was applied to a Mightysil-RP-18 (3-μm particle, Kanto Chemical, Osaka, Japan) frit-less column (45 mm × 0.150 mm i.d.) and separated using a 0–40% gradient of acetonitrile containing 0.1% formic acid over 80 min at a flow rate of 50 or 25 nl/min. Eluted peptides were sprayed directly into a quadrupole time-of-flight hybrid mass spectrometer (Q-Tof 2, Micromass Wythenshawe, UK). MS/MS spectra were acquired by data-dependent collision-induced dissociation, and MS/MS data were analyzed using the MASCOT software (Matrix Science, London, UK) for peptide assignment. The criteria were in accordance with the manufacturer's definitions. If necessary, match acceptance of automated batch processes was confirmed by manual inspection of each set of raw MS/MS spectra in which the major product ions were matched with theoretically predicted product ions from the data base-matched peptides. Proteins in the mock eluate from anti-FLAG antibody with FLAG-peptide were analyzed by the same LC-MS/MS method as used for the fibrillarin-associated complexes and then subtracted from the proteins identified in the total fibrillarin-associated complexes. Thus, those proteins identified in the mock eluate were not included in the fibrillarin-associated proteins unless the quantitative increase was confirmed.

Ultracentrifugation of FIB-associated RNP Complexes—The anti-FLAG immunoprecipitate obtained from FLAG-tagged FIB gene-transfected 293EBNA cells after elution with the FLAG peptide was analyzed on a 12–50% sucrose gradient in 50 mM Tris, pH 7.5, 25 mM KCl, 5 mM $MgCl_2$. The gradients were centrifuged in an SW65 rotor at 50,000 rpm (180,000 × *g*) for 3 h at 4 °C. A total of 18 fractions of 300 μl each were collected. The migration of the 40 S/60 S/80 S ribosomal complexes was determined by comparison to the ultraviolet absorption profile of cytosolic ribosomes fractionated by ultracentrifugation under identical experimental conditions.

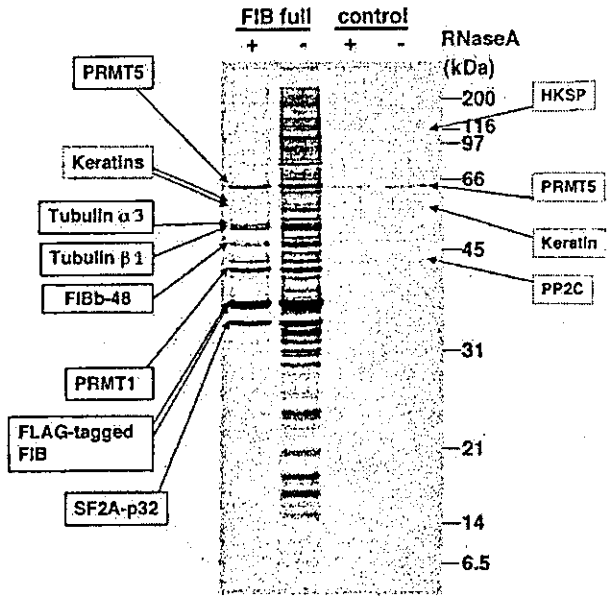

FIG. 2. **Protein components of immunoprecipitated FLAG-FIB-associated complexes and RNA dependence of binding to FIB.** Silver-stained 11% SDS-PAGE gel of FLAG-FIB-associated complexes immunoprecipitated with anti-FLAG after expression of FLAG-tagged full-length FIB. *Lanes 1* and *2*, FIB-associated complexes (*FIB full*) with (+) or without (−) RNase treatment; *lanes 3* and *4*, control immunoprecipitate with or without RNase. Molecular weight markers are indicated to the *right*. The protein bands identified by MALDI-TOF analysis after in-gel digestion of protein bands with protease are indicated on both sides of the gel. *Boxed proteins* denote FIB-associated proteins following RNase treatment. Proteins in *gray* indicate those identified in the control. *PRMT1* and *5*, protein arginine methyltransferases 1 and 5, respectively; *SF2A-p32*, splicing factor-2-associated protein p32; *FIBb-48*, FIB-binding protein 48 kDa; *HKSP*, kinesin-like spindle protein; *PP2C*, protein phosphatase 2C.

RESULTS

Isolation of FLAG-tagged FIB-associated Protein Complexes—Because endogenous FIB is found primarily in the nucleolus of mammalian cells, the subcellular localization of the FLAG-tagged protein in transfected 293EBNA cells was confirmed by immunofluorescence microscopy using an antibody to FLAG (Supplementary Fig. 1). Although weak staining was observed in the cytoplasm and nucleoplasm of the FLAG-FIB-transfected cells, the nucleolus exhibited intense staining thus confirming the correct localization of FLAG-tagged FIB.

Complexes associated with FIB were isolated from FLAG-FIB-transfected cells via immunoprecipitation using the FLAG antibody. A typical silver-stained SDS-PAGE gel of the immunoprecipitated fraction showed that FIB-associated complexes contained many proteins spanning a wide range of molecular weight (Fig. 2). In contrast, only four protein bands were apparent in a mock immunoprecipitate prepared from untransfected control cells (Fig. 2). In addition, when cells were transfected with unrelated FLAG-tagged proteins, an entirely different pattern of protein bands was obtained (data not shown). These results indicated that most of the factors immunoprecipitated from FLAG-FIB-transfected cells represented *de facto* FIB-associated proteins.

RNA Integrity in FIB-associated Complexes—RNA integrity is requisite for protein association in pre-rRNP complexes associated with human nucleolin, parvulin, and Nop56p, all of which may be involved in ribosome biogenesis as reported in our previous studies (25–27). Therefore, the requirement for RNA integrity was also analyzed for FLAG-FIB-associated complexes. RNase treatment prompted the dissociation of the

TABLE I

Putative fibrillarin-associated trans-acting factors involved in ribosome biogenesis

Accession number (GI) and calculated molecular mass are shown. Known function in mammals and yeast were extracted from the NCBI database entry and from the Saccharomyces Genome Database of Stanford University (genome-www.stanford.edu/Saccharomyces/) and David Tollervey's database (homepages.ed.ac.uk/dtoller/processing_components.html), respectively. For proteins that have yeast homologs, the gene names, open reading frame names, and percent identities with the homolog in overlapping amino acid regions are indicated.

Protein	Accession No. (GI)	MW (Da)	Function in mammals	Yeast Homolog	Yeast ORF	Percent identity to yeast homolog	Function in Yeast
Fibrillarin	11425985	33763.4	A component of a snRNP particle thought to participate in the first step of preribosomal RNA processing.	NOP1	YDL014W	66	35S primary transcript processing; rRNA modification.
Nucleolar protein 5A (56 kDa with KKE/D repeat)	12832025	66008.7	Similar to *S. cerevisiae* Sik1p, a nucleolar KKE/D repeat protein involved in pre-rRNA processing.	SIK1(NOP56)	YLR197W	50	35S primary transcript processing; rRNA modification.
Nucleolar protein NOP5/NOP58	7706254	59540.5	Putative snoRNA binding protein	NOP58	YOR310C	47	35S primary transcript processing; rRNA modification.
NHP2 non-histone chromosome protein 2-like 1 (S. cerevisiae)	4826860	14164.6	Binds to the 5' stem-loop of U4 snRNA. Nucleolar protein that associates with the checkpoint protein RAD17; highly similar to *S. cerevisiae* Snu13p.	SNU13	YEL026W	71	Pre-mRNA splicing factor; part of small (ribosomal) subunit (SSU) processosome (contains U3 snoRNA).
Splicing factor, arginine/serine-rich 4	5032089	56759.3	mRNA splicing; Splicing factor 4; member of the SR protein family; has an RNA recognition motif (RRM).	SRP40	YKR092C	32	Nucleocytoplasmic transport; Nopp140 homolog, a nonribosomal protein of the nucleolus and coiled bodies; nucleolar protein.
Hypothetical protein FLJ10774	12697963	116025.8	-	KRE33	YNL132W	55	40S subunit assembly and export to cytoplasm; killer toxin resistance.
Hypothetical protein FLJ10534	8922496	75069.7	Unknown	TSR1	YDL060W	32	-
Hypothetical protein AD034	13899340	64594.2	Unknown	RIO1/RRP10	YOR119C	38	20S pre-rRNA processing
DEAD/H (Asp-Glu-Ala-Asp/His) box polypeptide 5 (RNA helicase, 68 kDa)	4758138	69104.7	RNA helicase p68	DBP2	YNR112W	56	RNA helicase
DEAD/H box polypeptide 21	2135315	89195.5	RNA helicase Gu	DBP3	YGL078C	32	RNA helicase; 35S primary transcript processing; large ribosomal subunit assembly and maintenance.
Poly(A) binding protein, cytoplasmic 1	3183544	70625.9	Poly(A) binding	PAB1	YER165W	54	Poly(A) binding
Poly(A) binding protein, cytoplasmic 4 (inducible form)	4504715	70738.1	RNA-binding protein, binds to the mRNA poly(A) tail; may play a role in translation and mRNA stability.	PAB1	YER165W	53	Poly(A) binding
Heterogeneous nuclear ribonucleoprotein U (scaffold attachment factor A)	14141163	90423.0	Binds RNA and scaffold attached region DNA; contains an RGG box domain; component of hnRNP complexes; may play a role in hnRNA structure or processing.	NOP3	YDR432W	37	Required for efficient 27S pre-rRNA processing. Nop3p shuttles between the nucleus and the cytoplasm.
Splicing factor, arginine/serine-rich 1 (splicing factor 2, alternate splicing factor)	5902076	27727.8	Splicing factor 10; essential for constitutive pre-mRNA splicing; member of the SR family; alternative splicing factor.	NOP3	YDR432W	26	Required for efficient 27S pre-rRNA processing. Nop3p shuttles between the nucleus and the cytoplasm.
Splicing factor, arginine/serine-rich 6	13653676	39563.4	Splicing factor	NOP3	YDR432W	25	Required for efficient 27S pre-rRNA processing. Nop3p shuttles between the nucleus and the cytoplasm.
Pescadillo homolog 1, containing BRCT domain (zebrafish)	7657455	67960.0	Plays a crucial role in cell proliferation and may be necessary for oncogenic transformation and tumor progression.	NOP7	YGR103W	39	rRNA processing
DKFZP564M182 protein	3668141	58096.6	-	CIC1	YHR052W	26	26S proteasome; ribosome biogenesis.
Nucleolar GTPase	12652715	83629.5	Nucleolar GTPase	NOG2	YNR053C	55	Nuclear/Nucleolar GTP-binding protein 2
Putative nucleotide binding protein, estradiol-induced	7657048	63528.4	Nucleotide binding	NUG1	YER006W	30	Nuclear GTPase
Nucleolin	4885511	76298.2	Ribosome biogenesis	NSR1	YGR159C	32	rRNA processing; small ribosomal subunit assembly.
RNA-binding region (RNP1, RRM) containing 2	4757926	58905.5	Nuclear protein that may be a splicing factor; contains motifs characteristic of splicing factors.	NSR1	YGR159C	23	
Ras-GTPase activating protein SH3 domain-binding protein 2	14916573	54077.8	Probable scaffold protein that may be involved in mRNA transport.	NSR1	YGR159C	25	

TABLE I—*continued*

Protein	Accession No. (GI)	MW (Da)	Function in mammals	Yeast Homolog	Yeast ORF	Percent identity to yeast homolog	Function in Yeast
Hypothetical protein DKFZp762N0610	7959201	60443.4	Unknown	SRM1	YGL097W	27	Nuclear export of rRNA
Nucleophosmin (nucleolar phosphoprotein B23, numatrin)	15214852	32588.8	Nucleophosmin (nucleolar phosphoprotein B23, numatrin, protein B23); RNA-binding nucleolar phosphoprotein.	-	-		-
Other RNA helicases							
DEAD/H box polypeptide 3	13514813	73226.0	RNA helicase	DED1	YOR204W	49	RNA processing
DEAD/H box polypeptide 9 (RNA helicase A, nuclear DNA helicase II; leukophysin)	3915658	140788.0	RNA helicase	-	YLR419W	30	Helicase
DEAD/H box polypeptide 17 (72 kDa)	5453840	72326.0	RNA helicase p72	DBP2	YNR112W	58	RNA helicase
DEAD/H box polypeptide 30	7662362	133854.5	DDX30	-	YLR419W	31	Helicase
DEAD/H box polypeptide 36	14730578	114703.8	DDX36; DEAD/H box polypeptide 36.	-	YLR419W	29	Helicase
Nucleolar protein GU2	13129006	62514.1	A DEAD box enzyme that may be involved in ribosomal RNA synthesis or processing.	DBP3	YGL078C	31	35S primary transcript processing

majority of the protein components of FLAG-FIB-associated complexes. However, at least four major protein-staining bands as well as several minor bands remained associated with FLAG-FIB after RNase treatment (Fig. 2). The four major protein bands appeared to exhibit approximate equivalent stoichiometry with respect to staining intensity and were representative of the more abundant proteins present in the non-RNase-treated complexes (Fig. 2, compare *lanes 1* and *2*). In addition, the proteins released by RNase treatment could not be distinguished from those present in the RNase-untreated complexes except for the four major protein bands and several minor protein bands that remained associated with FLAG-FIB after RNase treatment, as judged by SDS-PAGE analysis (data not shown). These results suggested that at least two distinct groups of proteins are present in FIB-associated complexes, one whose association is dependent on RNA integrity (the FIB-associated RNPs) and another that associates directly with FIB (independent of RNA integrity). However, it was uncertain as to whether these two groups of proteins were associated with each other or present independently.

Identification of Protein Components in FIB-associated RNPs—Given the involvement of FIB in ribosome biogenesis, we expected isolated FIB-associated RNP complexes to contain trans-acting factors involved in this process, as well as ribosomal proteins. We therefore identified the protein components of the FIB-associated RNPs. We previously described a highly sensitive "direct nano-flow LC-MS/MS" system to identify proteins in limited amounts of multiprotein complexes (30). Immunoisolated FIB-associated complexes were digested with Lys-C and analyzed directly using the nano-LC-MS/MS system. In addition to the criteria for match acceptance described under "Experimental Procedures," more stringent criteria were adopted to conclusively identify proteins. Namely, at least two different peptides had to be identified in a single nano-LC-MS/MS analysis, and/or at least one peptide had to be identified at least twice (with highly significant data base matching scores) among four separate analyses. A total of 1426 peptides were identified via sequence data base searches using the collision-induced dissociation spectra obtained from four nano-LC-MS/MS runs of a Lys-C digest of the FIB-associated complexes. These peptide data identified 170 proteins (excluding the bait protein and the proteins present in mock) that met our identification criteria. Although we do not exclude that some of the proteins identified may be nonspecifically associated proteins, we believe most of the protein components identified in the fibrillarin-associated complexes are specifically associated with fibrillarin. Of the 170 proteins, 73 were ribosomal proteins (43 from the large subunit and 30 from the small subunit; Supplementary Table SI) and 97 were non-ribosomal proteins (Supplementary Tables SII and SIII). Of the non-ribosomal proteins, 24 were assigned as probable trans-acting factors involved in ribosome biogenesis based on their homology to yeast proteins known or expected to be involved in ribosome biogenesis (Table I and Supplementary Table SII).

In addition to the putative trans-acting factors that were assigned, the FIB-associated complexes contained 68 more non-ribosomal proteins, including a number of RNA-binding proteins, splicing factors, DNA-topoisomerase, Myb-binding protein, components of DNA-dependent protein kinase, components of the signal recognition particle, nuclear matrix proteins as well as many hypothetical/unknown proteins (Supplementary Table SIII). Of these, at least 44 proteins reportedly localize to the nucleolus or the nucleus (31, 32) (Supplementary Table SIII).

Identification of Proteins Associated with FIB without RNA Integrity—The proteins that remained associated with FIB after the RNase treatment were identified by MALDI-TOF analysis after in-gel digestion of excised SDS-PAGE gel bands with trypsin. The identified proteins were SKB1 homolog (protein arginine-methyltransferase 5, PRMT5) (GI: 5174683; 18 peptides matched; 29.6% peptide coverage; mean error = −3.41 ppm), tubulin α3 (GI: 5174733; 9 peptides matched; 27.2% peptide coverage; mean error = −11.42 ppm), tubulin β1 (GI: 135448; 13 peptides matched; 33.3% peptide coverage; mean error = 0.70 ppm), PRMT1 (GI: 2499803; 16 peptides matched; 55.6% peptide coverage; mean error = −4.21 ppm), and splicing factor SF2-associated protein p32 (SF2A-p32) (GI:4502491; 8 peptides matched; 50.7% peptide coverage; mean error = −5.08 ppm) (Fig. 2). These proteins were also identified by nano-LC-MS/MS analysis of the isolated FIB-associated RNPs without

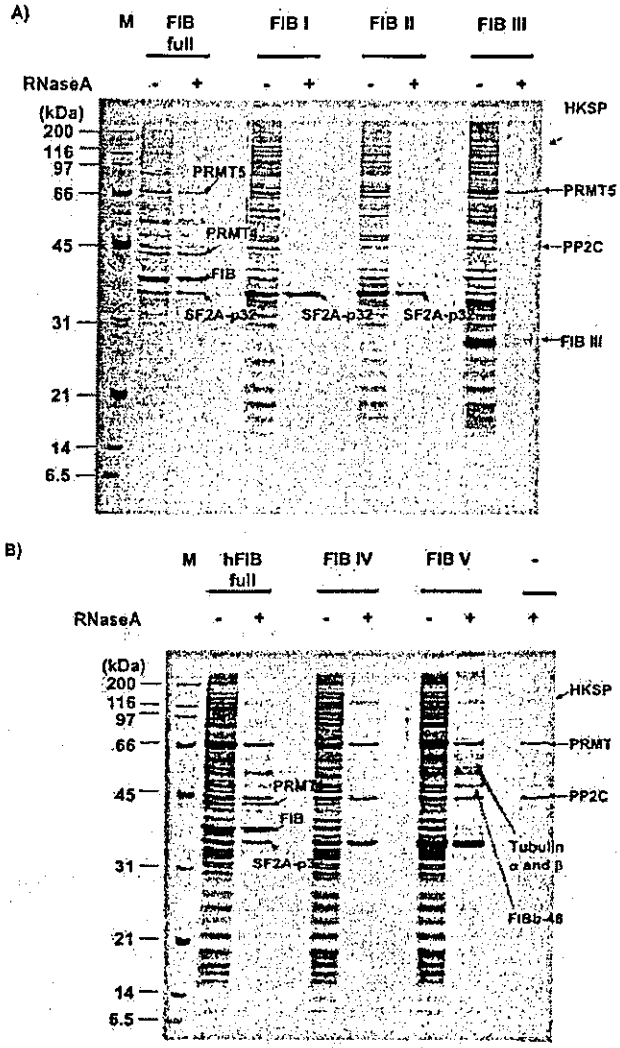

FIG. 3. **Protein components of immunoprecipitated FLAG-FIB- and truncated protein-associated complexes.** Silver-stained 11% SDS-PAGE gel of complexes immunoprecipitated with anti-FLAG after expression of full-length FIB or various truncation mutants. The *arrows* indicate the proteins that were identified. Abbreviations are as in Fig. 2. *A*, *Lane 1*, molecular weight markers; *lanes 2* and *3*, FIB-binding complexes (*FIB full*) with (+) and without (−) RNase treatment; *lanes 4* and *5*, FIB I-binding complexes with or without RNase; *lanes 6* and *7*, FIB II-binding complexes with or without RNase; *lanes 8* and *9*, FIB III-binding complexes with or without RNase. *B*, *Lane 1*, molecular weight markers; *lanes 2* and *3*, FIB-binding complexes (*FIB full*) with or without RNase; *lanes 4* and *5*, FIB IV-binding complexes with or without RNase; *lanes 6* and *7*, FIB V-binding complexes with or without RNase; lane 8, control with (+) RNase treatment.

RNase treatment (Supplementary Table SIII). However, MALDI-TOF analysis failed to identify other minor protein bands, including FIBb-48 (see Fig. 2).

Given that the association of FIB with the above proteins was RNA-independent, they may interact directly with FIB. To clarify the interactions between FIB and these proteins, expression vectors for three FLAG-tagged FIB truncated mutants with nuclear and nucleolar localization signals were initially constructed (Fig. 1) and expressed in 293EBNA cells. Each of the truncated proteins was expressed predominantly in the nucleolus (Supplementary Fig. S1) and exhibited the expected molecular weight, although mutants FIB I and FIB II migrated as multiple bands on SDS-PAGE gels probably due to post-translational modification *in vivo* (Supplementary Fig. S2). The protein complexes associated with each of the truncated proteins expressed in the 293EBNA cells were purified by immunoprecipitation with anti-FLAG-conjugated beads. Silver staining of an SDS-PAGE gel showed that a number of proteins were present in each of the three immunoprecipitates, and many of the bands were common among the three isolated protein complexes as well as in the full-length FIB-associated complex. Still, some protein bands were present uniquely in each of the complexes (Fig. 3*A*). When the immunoprecipitates were treated with RNase A, only SF2A-p32 remained associated with in the FIB I- and FIB II-associated complexes, whereas only PRMT5 remained associated with the FIB III-associated complexes (Fig. 3*A*). This result showed that SF2A-p32 interacts directly with the FIB GAR domain and spacer region 1 and that PRMT5 interacts with the methyltransferase-like domain (Fig. 1). Although PRMT5 was also detected in a mock immunoprecipitate prepared from control cells, its level was clearly elevated upon expression of FIB III. Despite the binding of SF2A-32p and PRMT5 to the corresponding truncated proteins, the binding of PRMT1 and other proteins associated with full-length FIB was not detected.

Two additional FIB truncation mutant expression vectors were constructed. FIB IV contained sequences encoded by FIB I and II, whereas FIB V contained FIB II and III sequences (Fig. 1). Both FIB IV and FIB V were expressed in 293EBNA cells, although FIB IV suffered some degradation that was most likely due to proteolytic cleavage from the C terminus (Supplementary Fig. S2). Immunoisolation using anti-FIB showed that these two truncated mutants were also associated with a number of proteins, most of which became dissociated upon RNase A treatment as was the case for the other truncation mutants (Fig. 3*B*). As expected from the FIB I and FIB II results, FIB IV associated with only SF2A-p32. On the other hand, in addition to SF2A-p32, FIB V also associated with tubulin α3 and β1 as well as several other proteins, including one with the molecular mass of 48 kDa (FIBb-48; Fig. 3*B*). PRMT5 and PP2C were detected more strongly in the control (Fig. 3*B*) than in previous experiments (compare with Fig. 3*A*) due to the use of different lots of anti-FLAG M2 affinity gel (purchased from Sigma-Aldrich Chemical, Steinheim, Germany). However, densitometry analysis indicated that PRMT5 was clearly increased in FIB V-associated protein complexes (and full-length FIB-associated complexes) compared with the control; *i.e.* the staining intensities of PRMT5 after RNase treatment were 19,149 (arbitrary values) for full-length FIB, 12,776 for FIB IV, 20,046 for FIB V, and 7,634 for the control (Fig. 3*B*). These results support the assertion that the methyltransferase-like domain corresponding to the FIB III mutant is responsible for the binding of FIB to PRMT5. These results also indicate that the presence of both the spacer region 1 and the methyltransferase-like domain is required for the binding of FIB to tubulin α3 and β1 as well as FIBb-48. With respect to the association of FIB with PRMT1, none of the five FIB truncation mutants bound this protein indicating that its binding is dependent on the domain structure of full-length FIB and/or that the binding of the other proteins (*e.g.* SF2A-p32 and PRMT5) is a prerequisite to PRMT1 binding. Together, these results suggest that FIB along with SF2A-p32, PRMT5, tubulins α3 and β1, FIBb-48, and PRMT1 constitute a subcomplex that functions as an integrated module.

Fractionation of FIB-associated RNP Complexes by Ultracentrifugation—The above results did not address whether the sub-complex that resulted from RNase A treatment constituted a protein complex that was independent of FIB-associated RNPs. Therefore, the immunoisolated FIB-associated complexes were fractionated by ultracentrifugation through a su-

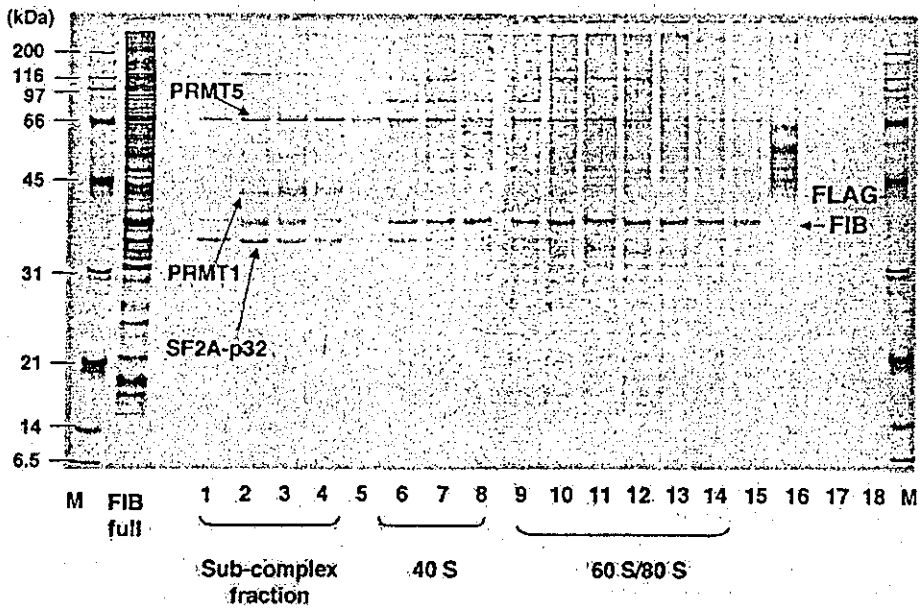

FIG. 4. **Separation of the FIB-associated sub-complex and RNP complexes by ultracentrifugation through a sucrose gradient.** FLAG-tagged FIB gene-transfected 293EBNA cells were subjected to immunoprecipitation using anti-FLAG. The immunoprecipitate was fractionated into 18 fractions by ultracentrifugation on a 12–50% sucrose gradient. The *arrow* below the SDS-PAGE gel indicates the fraction containing the sub-complex. Molecular weights are indicated to the *left*. *M*, molecular weight markers; *FIB full*, components of the immunoprecipitate loaded onto the gradient. Abbreviations are as in Fig. 2.

crose gradient and collected into 18 fractions, each of which was analyzed by SDS-PAGE (Fig. 4). Although FLAG-FIB was observed in nearly all the fractions, its distribution was concentrated in three peaks corresponding to 60 S/80 S ribosomes, 40 S ribosomes and sub-complexes. The majority of FIB was present in largest RNP complexes in the gradient (fractions 9–14). The proteins that were previously shown to remain associated with FIB after RNase treatment were found mostly in the sub-complex fractions (fractions 1–4), indicating that these RNA-independent FIB-associated proteins constitute an independent module. Thus, FIB forms a sub-complex that is primarily independent of the rest of the FIB-associated RNPs. Given that different patterns of protein bands were evident in the different fractions, the protein composition of the sub-complex may be somewhat heterogeneous.

DISCUSSION

FIB-associated protein complexes contain a number of ribosomal proteins and potential trans-acting factors involved in ribosome biogenesis, and the complexes are dependent on RNA integrity. Given the involvement of FIB in pre-rRNA methylation and processing, we conclude that, along with the sub-complex containing SF2A-p32 and PRMTs, the isolated FIB-associated protein complexes contain pre-rRNP complexes involved in ribosome biogenesis. The FIB-associated pre-rRNPs contain mainly 60 S-processing and assembly factors but also contain some 40 S factors suggesting that FIB pre-RNPs most likely form at early to middle stages of 60 S large subunit biogenesis (Table I) (33, 34).

One of the notable findings of this study is the RNA-independent association of FIB with SF2A-p32, PRMT5, tubulin α3, tubulin β1, FIBb-48kD protein, and PRMT1. SF2A-p32 binds the FIB GAR domain (corresponding to truncation mutant FIB I) and the spacer region 1 (FIB II), whereas PRMT5 binds the methyltransferase-like domain (FIB III) (Fig. 3). Given that FIB V, but not the FIB III, associated with tubulin α3, tubulin β1, and FIBb-48 protein (Fig. 3), both the methyltransferase-like domain and the spacer region 1 are necessary for the association of these proteins with FIB. However, the methyltransferase-like domain and the spacer region 1 were still not sufficient to recruit PRMT1. These results indicate that, in addition to these regions, the FIB GAR domain is required for the association with PRMT1. However, the data do not address whether PRMT1 binding is dependent on the recruitment of SF2A-p32, PRMT5, and the other proteins to FIB. Because these FIB-associated proteins fractionated as a much smaller complex relative to the FIB-associated pre-rRNPs that likely represent a mixture of 40 S and 60S/80S preribosomal particles (Fig. 4), these results indicate that FIB and these associated proteins constitute a sub-complex that is independent of the larger FIB-associated pre-rRNP complexes.

The association of FIB with two protein arginine methyltransferases is very intriguing, because FIB itself is an RNA methyltransferase. Thus, the association provides for the possible coordinated regulation of RNA and protein methylation events such as those in which both the RNA and protein molecules are involved. Two types of arginine methyltransferases were identified as FIB-associated proteins. First, PRMT5 (originally identified as the Janus kinase binding protein 1, or JBP1) is a type II methyltransferase that catalyzes the formation of N^G-monomethylarginine and symmetric N^G,N'^G-dimethylarginine (35) and is the catalytic component of the methylosome that regulates snRNP assembly (36). The second enzyme, PRMT1, is the predominant type I methyltransferase in cells and catalyzes the formation of N^G-monomethylarginine and asymmetric N^G,N^G-dimethylarginine (35). Thus, given that FIB is involved in ribosome biogenesis and is itself an RNA methyltransferase, our results provide biochemical evidence that these three different types of methyltransferases physically associate and therefore may function in concert. Given that, during ribosome biogenesis, not only are pre-rRNAs methylated but several nucleolar and ribosomal proteins as well (37–39), three types of methylation reactions may be required to coordinate certain stages of ribosome biogenesis and/or related processes.

FIB is known to interact with SMN protein (19), and we found that FIB interacts with PRMT5 (JBP1). Because SMN

protein is cooperated with PRMT5 in the methylosome complex during snRNP biogenesis (40), the result coupled with the fact that FIB interacts directly with SMN and co-localizes with SMN in Cajal bodies suggests that FIB may also participate in the regulatory mechanism by which the methylosome and the SMN complex mediate snRNP assembly. Thus, the protein- and RNA-methylation reactions may also occur simultaneously within very close proximity on a single molecular scaffold during snRNP biogenesis.

Another intriguing finding of this study is that FIB also interacts with SF2A-p32, which regulates RNA splicing by inhibiting both the binding of splicing factor ASF/SF2 to pre-mRNA and the phosphorylation of ASF/SF2 (41). Because it may compete with ASF/SF2 for SF2A-p32 binding, mRNA splicing may also be regulated by FIB.

In addition to SF2A-p32 and PRMTs, tubulins $\alpha 3$ and $\beta 1$ were also identified in the FIB-associated sub-complex. These microtubule subunits are heterodimers composed of one polypeptide each of α- and β-tubulin. Therefore, their presence in the sub-complex may provide a link to components of the microtubule cytoskeleton that consists of a highly organized network of microtubule polymers bound to accessory proteins, including microtubule-associated proteins, molecular motors, and microtubule-organizing proteins. Although no other components of microtubule cytoskeleton were found, the tubulins may be involved in transporting the FIB-associated sub-complex among subnuclear domains, including the nucleolus, nucleoplasm, and Cajal bodies.

Despite the preferable subcellular localization of FIB in Cajal bodies, its role in Cajal bodies is completely unknown. However, our results provide some clues on the possible roles of FIB in sn(o)RNP biogenesis and pre-mRNA processing in Cajal bodies. In addition, our finding that FIB associates with protein-arginine methyltransferases is also consistent with the recent report that symmetrical dimethylation of arginine is required to localize SMN to Cajal bodies as well as for its involvement in pre-mRNA splicing (42). FIB may function as a transporter of protein-arginine methyltransferases to Cajal bodies and/or as a scaffold to perform coordinated methylation of both RNA and protein substrates during RNA editing in Cajal bodies as well as in ribosome biogenesis in the nucleolus.

REFERENCES

1. Warner, J. R. (1990) *Curr. Opin. Cell Biol.* **2**, 521–527
2. Eichler, D. C., and Craig, N. (1994) *Prog. Nucleic Acids Res. Mol. Biol.* **49**, 197–239
3. Snaar, S., Wiesmeijer, K., Jochemsen A, G., Tanke, H. J., and Dirks, R. W. (2000) *J. Cell Biol.* **151**, 653–662
4. Spector, D. L. (2001) *J. Cell Sci.* **114**, 2891–2893
5. Smith, C. M., and Steitz, J. A. (1997) *Cell* **89**, 669–672
6. Kiss-Laszlo, Z., Henry Y., Bachellerie J. P., Caizergues-Ferrer, M., and Kiss, T. (1996) *Cell* **85**, 1077–1088
7. Tycowski, K. T., Smith, C. M., Shu, M. D., and Steitz, J. A. (1996) *Proc. Natl. Acad. Sci. U. S. A.* **93**, 14480–14485
8. Tyc, K., and Steitz, J. A. (1989) *EMBO J.* **8**, 3113–3119
9. Baserga, S. J., Yang, X. D., and Steitz, J. A. (1991) *EMBO J.* **10**, 2645–2651
10. Omer, A. D., Ziesche, S., Ebhardt, H., and Dennis, P. P. (2002) *Proc. Natl. Acad. Sci. U. S. A.* **99**, 5289–5294
11. Schimmang, T., Tollervey, D., Kern, H., Frank, R., and Hurt, E. C. (1989) *EMBO J.* **8**, 4015–4024
12. Henriquez, R., Blobel, G., and Aris, J. P. (1990) *J. Biol. Chem.* **265**, 2209–2215
13. Lapeyre, B., Mariottini, P., Mathieu, C., Ferrer, P., Amaldi, F., Amalric, F., and Caizergues-Ferrer, M. (1990) *Mol. Cell Biol.* **10**, 430–434
14. Aris, J. P., and Blobel G. (1991) *Proc. Natl. Acad. Sci. U. S. A.* **88**, 931–935
15. Jansen, R. P., Hurt, E. C., Kern, H., Lehtonen, H., Carmo-Fonseca, M., Lapeyre, B., and Tollervey, D. (1991) *J. Cell Biol.* **113**, 715–729
16. Turley, S. J., Tan, E. M., and Pollard, K. M. (1993) *Biochim. Biophys. Acta* **1216**, 119–122
17. David, E., McNeil, J. B., Basile, V., and Pearlman, R. E. (1997) *Mol. Biol. Cell* **8**, 1051–1061
18. Tollervey, D., Lehtonen, H., Jansen, R., Kern, H., and Hurt, E. C. (1993) *Cell* **72**, 443–457
19. Jones, K. W., Gorzynski, K., Hales, C. M., Fischer, U., Badbanchi, F., Terns, R. M., and Terns, M. P. (2001) *J. Biol. Chem.* **276**, 38645–38651
20. Wehner, K. A., Ayala, L., Kim, Y., Young, P. J., Hosler, B. A., Lorson, C. L., Baserga, S. J., and Francis, J. W. (2002) *Brain Res.* **945**, 160–173
21. Nicol, S. M., Causevic, M., Prescott, A. R., and Fuller-Pace, F. V. (2000) *Exp. Cell Res.* **257**, 272–280
22. Wang, H., Boisvert, D., Kim, K. K., Kim, R., and Kim, S. H. (2000) *EMBO J.* **19**, 317–323
23. Lischwe, M. A., Cook, R. G., Ahn, Y. S., Yeoman, L. C., and Busch, H. (1985) *Biochemistry* **24**, 6025–6028
24. Lischwe, M. A., Ochs, R. L., Reddy, R., Cook, R. G., Yeoman, L. C., Tan, E. M., Reichlin, M., and Busch, H. (1985) *J. Biol. Chem.* **260**, 14304–14310
25. Yanagida, M., Shimamoto, A., Nishikawa, K., Furuichi, Y., Isobe, T., and Takahashi, N. (2001) *Proteomics* **1**, 1390–1404
26. Fujiyama, S., Yanagida, M., Hayano, T., Miura, Y., Uchida, T., Fujimori, F., Isobe, T., and Takahashi, N. (2002) *J. Biol. Chem.* **277**, 23773–23780
27. Hayano, T., Yanagida, M., Yamauchi, Y., Shinkawa, T., Isobe, T., and Takahashi, N. (2003) *J. Biol. Chem.* **278**, 34309–34319
28. Hofer, L., Weichselbraun, I., Quick, S., Farrington, G. K., Bohnlein, E., and Hauber, J. (1991) *J. Virol.* **65**, 3379–3383
29. Goldfarb, D. S., Gariepy, J., Schoolnik, G., and Kornberg, R. D. (1986) *Nature* **322**, 641–644
30. Natsume, T., Yamauchi, Y., Nakayama, H., Shinkawa, T., Yanagida, M., Takahashi, N., and Isobe, T. (2002) *Anal. Chem.* **74**, 4725–4733
31. Andersen, J. S., Lyon, C. E., Fox, A. H., Leung, A. K. L., Lam, Y. W., Steen, H., Mann, M., and Lamond, A. I. (2002) *Curr. Biol.* **12**, 1–11
32. Scheri, A., Coute, Y., Deon, C., Calle, A., Kindbeiter, K., Sanchez, J.-C., Greco, A., Hochstrasser, D., and Diaz, J.-J. (2002) *Mol. Biol. Cell* **13**, 4100–4109
33. Nissan, T. A., Bassler, J., Petfalski, E., Tollervey, D., and Hurt, E. (2002) *EMBO J.* **21**, 5539–5547
34. Takahashi, N., Yanagida, M., Fujiyama, S., Hayano, T., and Isobe, T. (2003) *Mass Spectrom. Rev.* **22**, 287–317
35. Gary, J. D., and Clarke, S. (1998) *Prog. Nucleic Acids Res. Mol. Biol.* **61**, 65–131
36. Friesen, W. J., Paushkin, S., Wyce, A., Massenet, S., Pesiridis, G. S., Van Duyne, G., Rappsilber, J., Mann, M., and Dreyfuss, G. (2001) *Mol. Cell Biol.* **21**, 8289–8300
37. Pintard, L., Kressler, D., and Lapeyre, B. (2000) *Mol. Cell Biol.* **20**, 1370–1381
38. Niewmierzycka, A., and Clarke, S. (1999) *J. Biol. Chem.* **274**, 814–824
39. Whitehead, S. E., Jones, K. W., Zhang, X., Cheng, X., Terns, R. M., and Terns, M. P. (2002) *J. Biol. Chem.* **277**, 48087–48093
40. Pellizzoni, L., Yong, J., and Dreyfuss, G. (2002) *Science* **298**, 1775–1779
41. Petersen-Mahrt, S. K., Estmer, C., Ohrmalm, C., Matthews, D. A., Russell, W. C., and Akusjavi, G. (1999) *EMBO J.* **18**, 1014–1024
42. Boisvert, F. M., Cote, J., Boulanger, M. C., Cleroux, P., Bachand, F., Autexier, C., and Richard, S. (2002) *J. Cell Biol.* **159**, 957–969

CHAPTER 24

Combining Surface Plasmon Resonance with Mass Spectrometry: Identifying Binding Partners and Characterizing Interactions

Jos Buijs* and Tohru Natsume†

**Biacore AB, Rapsgatan 7, 75450 Uppsala Sweden; †National Institute of Advanced Industrial Science and Technology. Biological Information Research Center, 2-41-6 Ohmi, Kohtoh-ku, Tokyo 135-0064, Japan*

OPTICAL BIOSENSORS HAVE COME TO BE WIDELY USED in many fields since their introduction as a research tool for the characterization of macromolecular interactions. One of the most prominent uses of biochemical sensing exploits surface plasmon resonance (SPR), a phenomenon that has been known for more than 30 years (Kretschmann 1971). For recent reviews of SPR (Winzor 2003), and its applications to proteomics, see Natsume et al. (2001).

SURFACE PLASMON RESONANCE BIOSENSORS

The central component of an SPR biosensor (as illustrated in Figure 24.1) is the sensor chip, a glass slide with a prism mounted on one side and a thin metal coating on the other side. Bait molecules are immobilized on the metal coating, most commonly in a carboxymethylated dextran film, and exposed to potential binding partners in the flow channel. A mono-

chromatic polarized light beam is directed at the sensor chip from various angles through the prism. At certain angles of incidence, the beam is totally internally reflected, and the reflected beam is detected by a sensor (the optical detection unit). When the incident beam is reflected, it produces an evanescent wave that penetrates the aqueous medium on the other side of the chip. Penetration depth is on the order of one wavelength. At a specific angle of incidence, a resonant coupling occurs between the evanescent wave and the surface plasmons. The plasmons absorb energy from the wave, causing a reduction in the intensity of the reflected beam, which can be recorded by an optical density unit. The coupling depends only on the angle of incidence and the refractive index of the medium penetrated by the evanescent wave. Changes in the density, and hence the refractive index, of the aqueous medium occur when analytes in the flow channel bind to bait molecules on the chip. This causes SPR to occur at a different angle of incidence. A sensogram, plotting resonance units against time, provides a real-time quantification of the interaction between bait and target. Application of this approach in affinity-based biosensing is discussed by Jönsson et al. (1991) and Nagata and Handa (2000). There have been several types of SPR instruments (Ward and Winzor 2000); however, this chapter describes experiments using Biacore, as it is the most commonly used instrument.

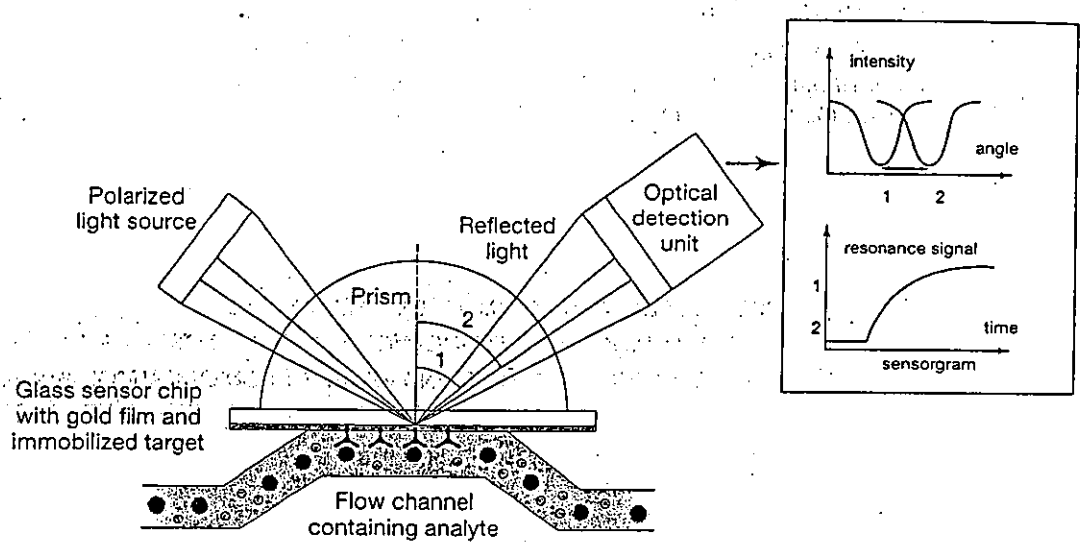

FIGURE 24.1. Schematic picture of an SPR biosensor. The polarized light is focused into a wedge-shaped light beam that illuminates the sensor chip under conditions of total internal reflection. Under these conditions, SPR results in a reduction in the intensity of light reflected from the sensor surface at a specific angle. A plot of reflected intensity against the angle shows a characteristic "dip" (*upper panel*). The angle of minimum reflectance is called the resonance angle. The resonance angle varies as a function of the refractive index of the medium near the sensor surface. A molecule (e.g., an antibody) is immobilized on the sensor chip and a sample containing a binding partner (e.g., antigen) is delivered over the sensor surface. Binding between the partners leads to an increase in the mass concentration, resulting in an increase in the refractive index and a shift in the position of the resonance angle (from 1 to 2 in the figure). The changes in the resonance angle over time are displayed in a graph called a sensorgram (*lower panel*), which is the direct representation of the interaction between the molecules on the sensor surface in real time. The unit for the SPR signal is the resonance unit (RU), where 1000 RU represents a shift in the resonance angle of 0.1°. Also note that the samples are in contact with the IFC channel in the microfluidics. To minimize the loss of the protein by adsorption to the wall of the vials or the IFC channel, use the urea-containing recovery buffer.

LIGAND FISHING AND IDENTIFICATION USING SPR BIOSENSOR AND MASS SPECTROMETRY

SPR biosensors are primarily used to characterize biomolecular interactions and are amenable to high-throughput analysis for the following reasons:

- Analysis is label-free and performed in real time, thus avoiding detection time lags.
- An auto-sample injection system allows large numbers of samples to be processed simultaneously.

The microfluidics technology incorporated into the sensor chips allows SPR to be detected in very small sample volumes (μl). SPR biosensors have been used effectively for "ligand fishing," identifying interactions between target molecules and candidate ligands (Lackmann et al. 1996; Sakano et al. 1996; Seok et al. 1997; Markgren et al. 1998; Iemura et al. 1999; Williams 2000). Unfortunately, when a binding partner is found in a biological mixture, the task of identifying the ligand is daunting. Purification of the ligand can be time-consuming and labor-intensive, often requiring the use of tailor-made strategies.

To facilitate ligand identification, SPR detection can be combined with affinity chromatography (see Chapters 10–12) and mass spectrometry (MS) (see Chapter 21 and for additional information, see Chapter 8 of Simpson 2003). MS is one of the most sensitive and specific techniques available for the identification and characterization of biomolecules. The following are two ionization mechanisms that are commonly used for MS.

- Matrix-assisted laser desorption/ionization (MALDI), in which proteins, crystallized on a sample support, are ionized by laser irradiation.
- Electrospray ionization (ESI), in which ions are generated directly from solution.

Identification of biomolecules after affinity purification with SPR biosensors has been demonstrated using both ESI-MS (Natsume et al. 2000, 2001) and MALDI-MS (Sönksen et al. 1998; Nelson and Krone 1999; Williams and Addona 2000; Catimel et al. 2001; Natsume et al. 2002). By integrating chip-based affinity purification with SPR detection, it is possible to monitor binding kinetics directly, i.e., in what proportions the molecules bind, how quickly and how tightly they bind (association and dissociation constants), and under what conditions. By combining SPR detection with MS, the molecules captured on the sensor chip can be validated or confirmed in a high-throughput manner.

Recovering samples from SPR sensor chips has been possible for many years, but one of the commercial instruments, the Biacore 3000 (Biacore), has recently been upgraded, in both software and hardware (BR-1005-75, Biacore), to enhance protein recovery (Figure 24.2). The improvements have been made in the recovery of proteins, after affinity purification, for subsequent MS analysis.

The Biacore 3000 instrument is particularly useful for ligand-fishing experiments, in which it can be used to monitor the immobilization of a bait protein, to capture the target protein and recover it from the sensor chip, and, finally, to prepare the recovered material automatically for MS analysis. These experimental steps are described in detail in the Case Study described below. A list of sensor chips suitable for the affinity purification of proteins is given in Table 24.1.

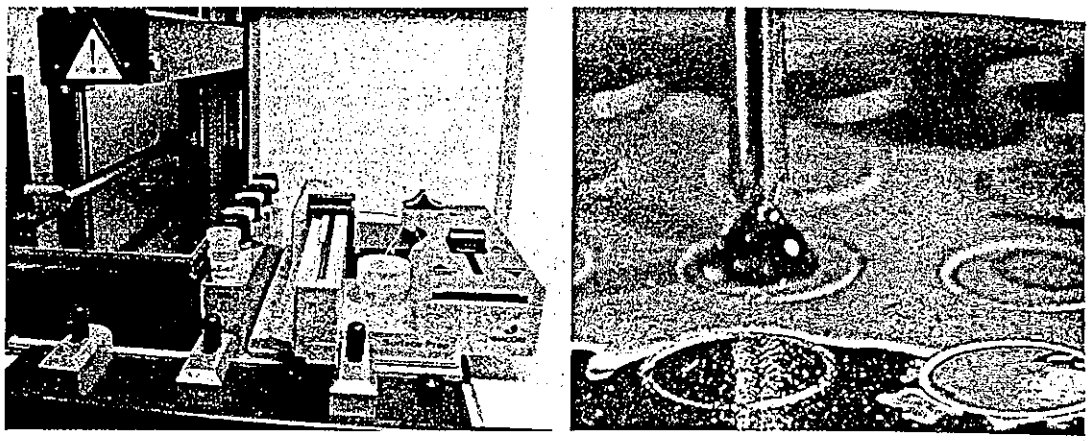

FIGURE 24.2. The Biacore 3000 for MS analysis. A 3.3x larger surface area in the Surface Prep Unit enables more efficient capturing of the bound molecules. The recovered sample is automatically delivered to a vial or deposited directly to the MALDI target located in the auto sampler area on a MALDI target holder. The enzyme solution or matrix can be deposited onto the sample on the MALDI target.

CASE STUDY: LIGAND FISHING AND IDENTIFICATION OF CALMODULIN FROM BRAIN EXTRACT

In this example, an experiment was set up to capture calmodulin from bovine brain extract on the sensor chip. The captured protein was recovered and identified using peptide mass fingerprinting. The entire process—of affinity purification, recovery of calmodulin, and sample preparation for MS analysis, including enzymatic digestion on the MALDI target—was automated using the Biacore 3000.

Calmodulin is a ubiquitous Ca^{2+}-binding protein that is found in eukaryotic cells and functions as a major physiological effector for a wide range of cellular responses. Besides the regulation of intracellular Ca^{2+} levels, calmodulin is reported to have a role in the activation of nuclear protein importation, thereby establishing a link between signal transduction and nuclear import. Myosin light-chain kinase is one of the physiological interaction partners of calmodulin. A peptide derived from this protein, containing the calmodulin-binding domain, was used as bait for calmodulin.

The protocol used is detailed below with the experimental steps, as controlled by the Biacore 3000 software, summarized in Table 24.2. All experiments were performed at 25°C and the water used was obtained from a Milli-Q water purification system (Millipore).

TABLE 24.1. Sensor chips that can be used for affinity purification using the Biacore 3000 biosensor

Sensor Chip*	Surface Coating	Applications
CM5 (BR-1000-14)	carboxymethylated dextran	general purpose
NTA (BR-1000-34)	carboxymethylated dextran, preimmobilized with NTA	capture of histidine-tagged biomolecules
SA (BR-1000-32)	carboxymethylated dextran, preimmobilized with streptavidin	captures biotinylated biomolecules
CM4 (BR-1005-39)	carboxymethylated dextran with lower degree of carboxylation than CM5	reduces nonspecific binding of highly positively charged molecules as may be found in cell lysates

*Information in parentheses indicates Biacore catalog numbers.

TABLE 24.2. Sequential listing of the experimental steps for a ligand fishing experiment, including the utilized Biacore 3000 commands

Process	Command	Volumes, Solution, and Flow Rates
Equilibrate system with buffer	prime	HBS-EP
Surface activation	mix inject	100 µl of EDC with 100 µl of NHS 35 µl of EDC/NHS, 5 µl/min
CBD immobilization	inject	50 µl of CBD, 5 µl/min
Deactivation	inject	35 µl of EtAm, 5 µl/min
Condition	quickinject	10 times 5 µl of 50 mM NaOH, 5 µl/min
Change buffer	prime	3 times HBS-N
Injection of bovine brain extract	MS_inject	200 µl of brain extract, 20 µl/min, 200 µl of MS buffer
Wash	MS_wash	30 µl of NaOH, 40 µl of NaOH, 200 µl of MS buffer
Recovery	MS_recover	50 µl of recovery buffer, 250 µl of H_2O, 300 µl of MS buffer
Add	microtransfer	1 µl of trypsin
Digestion	wait 900	wait for 15 minutes
Add	microtransfer	1 µl of TFA
Add	microtransfer	1 µl of matrix solution

The type of solutions, their volumes, and if applicable, the flow rate at which solution is injected in the instrument are given in column 3.

MATERIALS

CAUTION: See Appendix 7 for appropriate handling of materials marked with <!>.

◗ Reagents

Calmodulin-binding domain (CBD) (0.1 mg) (CalBiochem)

EDC (1-ethyl-3-[3-dimethylaminopropyl] carbodiimide hydrochloride) (e.g., Sigma or Biacore) <!>

Ethanolamine-HCl (1 M, pH 9.0) (e.g., Sigma or Biacore) <!>

HBS-EP

- 10 mM HEPES (pH 7.4)
- 150 mM NaCl
- 3 mM EDTA
- 0.005% Surfactant P20

Surfactant P20 is polyoxyethylenesorbitan, a nonionic surfactant recommended for inclusion in the buffers used in Biacore systems. It is available from Biacore, where it has been tested for peroxides and carbonyls, and is supplied as a sterile-filtered 10% solution in water.

HBS-N: 10 mM HEPES containing 150 mM NaCl (pH 7.4)

HBS-N containing 2 mM $CaCl_2$ <!>

Initial buffer for microcolumn: 0.1% formic acid (100 µl required) <!>

Matrix solution

Dissolve 0.5 mg of α-cyano-4-hydroxycinnamic acid <!> (Bruker) in 670 µl of ethanol <!> and 330 µl of acetone <!>.

MS buffer: 50 mM ammonium bicarbonate <!> and 2 mM $CaCl_2$ (pH 8.2)
For MS-compatible buffers, see note in Stage 2.
NaOH (50 mM) <!>
N-hydroxysuccinimide (e.g., Sigma or Biacore) <!>
Aliquots (100 µl) of *N*-hydroxysuccinimide should be stored at –20°C.
Potassium phosphate buffer (10 mM, pH 7.4) <!>
Recovery solution: 0.5 mM EGTA and 50 mM NH_4HCO_3 (pH 8.2)
For recovery solutions, see note in Stage 3.
Running buffer
Trifluoroacetic acid (TFA) (0.5% v/v) <!>
Trypsin <!>, Sequence-grade modified (Promega), 15 µg/ml in 60% acetonitrile <!>
Wash solutions
For suitable wash solutions, see Step 9.

Equipment

Biacore 3000 instrument equipped with sample rack, autosampler, and software (version 4.0 or higher).
For information on analyte recovery using an earlier version of the Biacore 3000, contact Biacore directly (www.biacore.com).
CM5 sensor chip (Biacore)
MALDI target (e.g., Scout MTP, Bruker, ABI Voyager, MALDI-Qstar, Micromass Qtof)
If using the alternative procedure for Stage 4, the analyte is collected in a vial rather than being deposited on a MALDI target.
Mass spectrometer (e.g., Autoflex MALDI-TOF from Bruker)

Biological Sample

Bovine brain extract: 10 mg of bovine brain acetone powder (Sigma)

Additional Materials

The alternative Stage 4 of this protocol requires the following additional reagents:
Microcolumn 1 elution buffer: 30% acetonitrile <!>, 0.1% formic acid <!>
Microcolumn 2 elution buffer: 20 mg/ml sinapinic acid <!>, 60% acetonitrile, 0.1% trifluoroacetic acid <!>
For ESI-MS analysis
ESI or tandem mass spectrometer (ESI-LC-MS or ESI-LC-MS/MS)
Nanospray tip (e.g., nanoflow probe tip [Micromass]; nanobore stainless steel emitters and stage tips [Proxeon Biosystems A/S]; and PicoTips [New Objective, Inc.])
Formic acid (0.1% v/v) in H_2O
Incubator set at 37°C
For MALDI analysis
MALDI target
MALDI-TOF mass spectrometer
Sinapinic acid crystals (20 mg/ml sinapinic acid in acetone)
Micro-reversed-phase POROS column prepared in a GELoader tip according to the method of Gobom et al. (1999)
Trifluoroacetic acid (TFA) (50 nl)

Trypsin digestion buffer (pH 9.0): 100 mM Tris <!>, 4 M urea <!>, and 0.01% *n*-octylglucopyranoside
Trypsin (15 μg/ml) in trypsin digestion buffer
Trypsin, sequencing-grade (Promega)

METHOD

Stage 1: Immobilization of the CBD to a CM5 Sensor Chip

The CBD was immobilized to a carboxymethylated dextran of the sensor chip by amine coupling chemistry (see Johnsson et al. 1991). In this procedure, the molecules are covalently coupled via their primary amine groups to the sensor chip. The coupling provides the high degree of immobilization necessary for successful recovery experiments. The number of molecules captured on the chip is directly proportional to the degree of immobilization and the number of flow cells. In a Biacore 3000, four flow cells, each with a surface area of 1.2 mm^2, are available for this purpose.

1. Equilibrate the system with HBS-EP using the PRIME command.
2. Thaw 100-μl aliquots of EDC and NHS, vortex, and place them in the appropriate slots in the sample rack. Activate the sensor chip surface with 200 μl of a 1:1 mixture of these solutions using the MIX command.
3. Prepare a solution of CBD by dissolving 0.1 mg of CBD in 1 ml of 10 mM potassium phosphate buffer (pH 7.4) and divide it into 100-μl aliquots. INJECT 35 μl of EDC/NHS at a flow rate of 5 μl/min. Then INJECT 50 μl of CBD, at the same rate, over the activated sensor surface for coupling.
4. After coupling the CBD, deactivate excess active groups on the sensor surface by injecting 35 μl of ethanolamine at a flow rate of 5 μl/min. To condition the sensor, QUICKINJECT ten 5-μl aliquots of 50 mM NaOH at 5 μl/min.

Stage 2: Capturing Calmodulin (CaM) on the Sensor Chip

5. Prepare the bovine brain sample from bovine brain acetone powder by suspending 10 mg in 1 ml of HBS-N containing 2 mM $CaCl_2$. Centrifuge the extract at 16,000*g* (Biofuge pico, Heraeus Instr.) and discard the insoluble pellet. Dilute the supernatant 10 times in the same buffer.
6. After ~1 minute of running buffer flow, PRIME the system with three applications of HBS-N.

   The HBS-N is a low-salt MS-compatible buffer, which replaces the higher-salt running buffer (see the shaded panel below regarding MS-compatible buffers), as can be seen from the dip (at ~50 seconds) in the sensorgram shown in Figure 24.3. The dip occurs because the lower-salt buffer has a lower refractive index than the running buffer (see the section on Surface Plasmon Resonance Biosensors).

7. MS_INJECT 200 μl of brain extract (20 μl/min), followed by 200 μl of MS buffer over the CM5 chip immobilized with CBD.

   Generally, flow rates ranging from 1 to 20 μl/min and sample volumes on the order of a few tenths to hundreds of microliters are used to capture the target molecule.

8. Directly after sample injection, flush the integrated fluidic system (IFC), including the flow cell area, with an MS-compatible buffer (HBS-N) for 6 seconds.

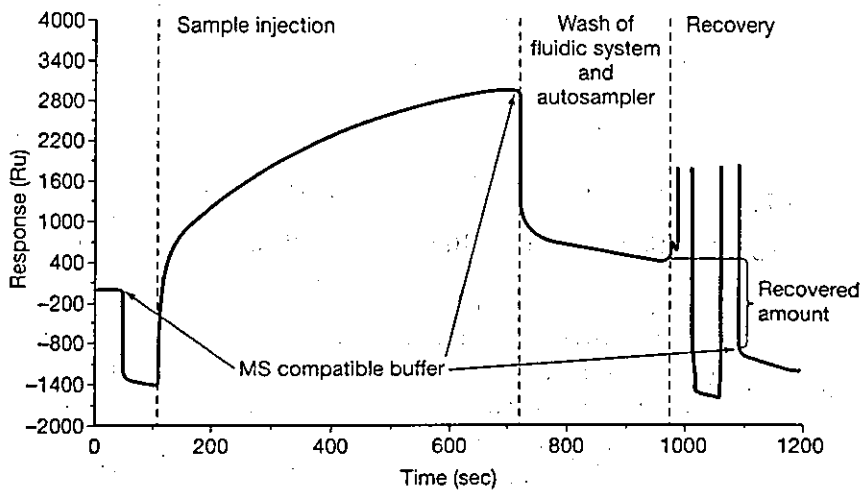

FIGURE 24.3. A typical sensorgram, showing the SPR signal (in response units, RU) during an affinity purification and recovery experiment. A signal of 1 RU in one flow cell corresponds to 1 pg of protein (see Stenberg et al. 1991).

MS-COMPATIBLE BUFFER

MS-compatible buffer is used throughout the affinity purification experiment. It is crucial for the MS sensitivity of the recovered sample and has three functions:

- It washes the flow cells when the target protein is captured on the chip.
- It separates carryover contamination from chemicals present in the running buffer and in the injected sample.
- It is used before and after the various steps in the affinity purification and recovery experiment to quantify bound and recovered levels from the sensorgram.

The MS-compatible buffer provides a suitable environment to maintain the integrity of the biomolecular interaction, but it contains as little salt as possible so that it does not interfere with the MS analysis. Volatile buffers such as ammonium bicarbonate are compatible with MS analysis as they evaporate during the MALDI sample preparation step. Buffers containing organic acids in combination with ammonium, such as ammonium acetate, citrate, or formate, are also compatible when used at lower concentrations. More common buffers can affect MS sensitivity in various ways. For a detailed list of the compatibility of buffers with MALDI-MS analysis, see Kallweit et al. (1996). Phosphate, for example, is known to have a strong negative effect, whereas other buffers, such as Tris and HEPES, are more compatible with MALDI-MS. The MS-compatible buffer in this experiment contains 50 mM ammonium bicarbonate and 2 mM $CaCl_2$. The $CaCl_2$ was added because Ca^{2+} is required for the binding of calmodulin to CBD.

By using a desalting micro-reversed-phase column (see below An Alternative Method for Stage 4: Sample Preparation for MS Analysis), even buffers that are incompatible with MS ionization can be used (for further information on desalting micro-reversed-phase columns, see Chapter 8 [including Protocol 2] of Simpson 2003). A chaotropic reagent such as urea can be added to denature recovered sample prior to digestion. (Some proteins can be digested only under denaturing conditions.) Urea-containing recovery buffer can also be used to minimize protein adsorption to the wall of the vial or the IFC channel (see Figure 24.1 and its legend), leading to more efficient recovery of low-abundance or sticky proteins.

Stage 3: Recovery of Calmodulin from the Sensor Chip

9. Wash the autosampler and IFC, but not the flow cells, sequentially with three solutions using the MS_WASH command, as follows.
   - Use a mild basic or acidic solution (e.g., 50 mM NaOH, 1–5% TFA, formic acid, or acetic acid) or low-concentration organic solvents (10–20% acetonitrile or methanol) for the first two wash solutions.
   - For the third wash, use an MS-compatible buffer to equilibrate the IFC prior to sample recovery.
10. Recover the bound calmodulin using the MS_RECOVER command, which applies 2 µl of recovery solution to the sensor chip, and incubate it for 30 seconds.
11. Draw the 2-µl portion back into the autosampler needle. For peptide fingerprinting, deposit the sample on a Scout MTP MALDI target (Bruker) with a spot size of 0.8 mm and continue with Stage 4 below. For material recovered in non-MS-compatible buffer, collect the sample in a vial and continue with the alternative Stage 4 procedure.

During the MS_RECOVER process, air is passed over the flow cells for 30 seconds before and after the recovery solution is incubated in the flow cells. When air is flowing through the flow cells, the SPR signal is temporarily disrupted, as seen in the sensogram (Figure 24.3).

RECOVERY SOLUTIONS

The selection of the recovery solution is directly related to the way in which the sample is prepared for MS analysis. MS analysis often requires acidification of the sample to generate abundant positively charged analytes. At the same time, low concentrations of organic acids, e.g., 0.5% TFA, are often suitable to release the captured target molecules from the sensor chip.

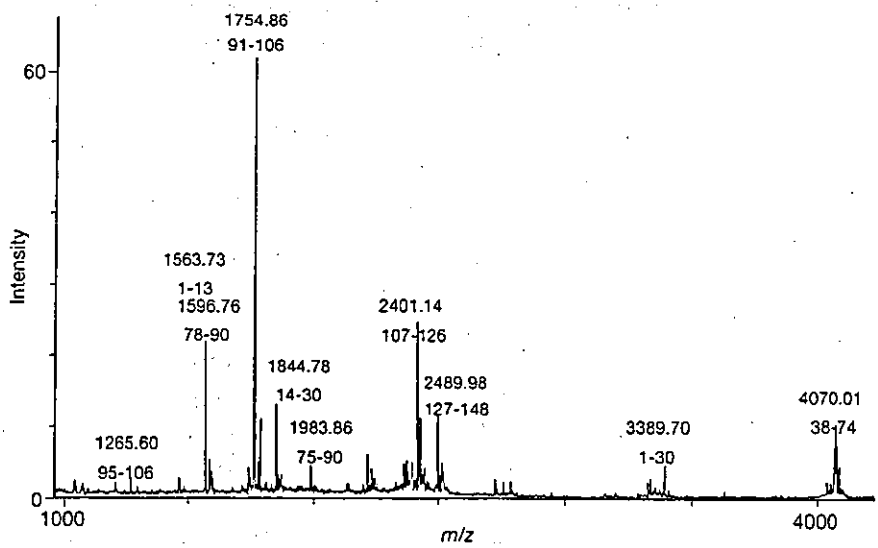

FIGURE 24.4. MALDI spectrum of a tryptic digest of the recovered target protein after injection of brain extract over a sensor chip, modified with the calmodulin-binding domain. The *m/z* values of these mass peaks were submitted to a database (Mascot; for details on searching databases using MS data, see Search Engines for Identifying Proteins Using MS Data in Chapter 8 of Simpson [2003]) and bovine calmodulin was unambiguously identified. The sequence coverage was 95%. Three peptide ions (1563.73, 2401.14, and 3389.70 *m/z*) were not identified in the first database search. Two additional peptides (1563.73 and 2401.14 *m/z*) were assigned when the posttranslational modifications were incorporated in the database correlation (acetylated amino terminus and trimethylated Lys-114).

Stage 4: Preparation of the Recovered Material for Mass Spectrometry Analysis

12. For peptide mass fingerprinting, digest the target protein on the MALDI plate with trypsin prior to adding the matrix. Use the MICROTRANSFER command to add 1 µl of trypsin (15 µg/ml in 60% acetonitrile) to the recovered material (final concentration 5 µg/ml) on the MALDI target. Allow it to dry (~15 minutes, use the WAIT 900 command).

    For additional details on preparing samples for peptide mass fingerprinting, see Chapters 8 and 9 (including Protocol 3) in Simpson (2003).

13. After digestion, acidify the sample using the MICROTRANSFER command to add 1 µl of TFA (0.5% v/v) and then 1 µl of a matrix solution.

14. Record mass spectra using a mass spectrometer in the reflection mode with delayed extraction, and submit the *m/z* values of the mass peaks to a database.

    A typical mass spectrum and database search is shown in Figure 24.4. For details on searching databases using MS data, see Search Engines for Identifying Proteins Using MS Data in Chapter 8 of Simpson (2003).

IMPORTANT

- As matrix solutions tend to leave crystals on the autosampler needle, an additional wash of the needle in organic solvents may be necessary.
- General guidelines for MALDI sample preparations, including digestion, are described by Kussmann and Roepstorff (2000). Note that the ionization process in MS measurements is extremely sensitive to contaminants such as detergents (SDS, Tween), buffer salts, and even leakage of chemical substances from column material and vials. In cases where these problems occur, samples should be cleaned up using a micro-reversed-phase column (see below An Alternative Method for Stage 4: Sample Preparation for MS Analysis; also for further information on desalting micro-reversed-phase columns, see Chapter 8 [including Protocol 2] in Simpson 2003).

An Alternative Method for Stage 4: Sample Preparation for MS Analysis

When samples are recovered in a vial, instead of being deposited on a MALDI target, it is important to minimize the delay between their recovery and their preparation for MS. Proteins stick to almost all surfaces with which they come in contact. Because of the small volumes and low concentrations used, losses through adsorption and sample handling can be significant. Adsorption can be avoided by adding urea and *n*-octylglucopyranoside (an MS-compatible detergent) to the recovery buffer. If this proves to be necessary, samples must also be cleaned up and desalted prior to MS analysis. The $ZipTip_{micro\text{-}C18}$ (Millipore) is a column suitable for cleaning up, concentrating, and desalting samples; samples can be eluted in as little as 0.5 µl of solution. Even smaller elution volumes (down to 50–100 nl) are possible using a homemade POROS reversed-phase (ABI) microcolumn constructed inside a GELoader tip (Eppendorf) (see Gobom et al. 1999; Simpson 2003). Samples recovered from these columns in non-MS-compatible buffer can be analyzed using MALDI or ESI-MS. The following procedure describes the preparation of material recovered in a non-MS-compatible buffer.

METHOD

1. Digest the target protein with trypsin by adding 1 µl of 15 µg/ml trypsin in trypsin digestion buffer to the vial. Incubate for 2 hours at 37°C.

2. Desalt the digestion mixture and concentrate the sample using a micro-reversed-phase POROS column. Equilibrate the column with 0.1% formic acid (FA) in H_2O (initial buffer), and pass the trypsin digestion mixture over the column. Then wash the column with the same initial buffer.

   IMPORTANT: Due to the high back pressure, the micro-reversed-phase POROS packing is the only one recommended.

3. Complete one of the two following procedures.

   For ESI-MS analysis:

   a. Elute the peptide mixture in 0.5–1 µl of Microcolumn 1 elution buffer.

   b. Load the sample into the capillary using either a fused silica syringe needle or a gel loader tip. Apply pressure to the back of the tip until a drop of liquid is seen.

   c. Tune the source voltage, and adjust the gas flow for maximum ion current. Record mass spectra. For details of the operation, see Wilm and Mann (1996).

   For MALDI analysis:

   a. Elute the peptide mixture in 50 nl of Microcolumn 2 elution buffer, directly onto a nano-spray tip.

   b. Cover the deposited sample with a thin layer of sinapinic acid crystals (20 mg/ml sinapinic acid in acetone).

   c. Record mass spectra using a MALDI-TOF mass spectrometer according to the manufacturer's instructions.

ACKNOWLEDGMENTS

We thank A. Zhukov and Ö. Jansson for their contributions in developing the recovery functionality in the Biacore 3000 and for experimental data, and S. Hashimoto for editing the manuscript.

REFERENCES

Catimel B., Rothacker J., and Nice E. 2001. The use of biosensors for microaffinity purification: An integrated approach to proteomics. *J. Biochem. Biophys. Methods* 49: 289–312.

Gobom J., Nordhoff E., Mirgorodskaya E., Ekman R., and Roepstorff P. 1999. Sample purification and preparation technique based on nano-scale reversed-phase columns for the sensitive analysis of complex peptide mixtures by matrix-assisted laser desorption/ionization mass spectrometry. *J. Mass Spectrom.* 34: 105–116.

Iemura S., Yamamoto T.S., Takagi C, Kobayashi H., and Ueno N. 1999. Isolation and characterization of bone morphogenetic protein-binding proteins from the early *Xenopus* embryo. *J. Biol. Chem.* 274: 26843–26849.

Johnsson B., Löfås S., and Lindquist G. 1991. Immobilization of proteins to a carboxymethyldextran modified gold surface for biospecific interaction analysis in surface plasmon resonance. *Anal. Biochem.* 198: 268–277.

Jönsson U., Fagerstam L., Ivarsson B., Johnsson B., Karlsson R., Lundh K., Löås S., Persson B., Roos H., and Rönnberg I., Sjölander S., Stenberg E., Ståhlberg R., Urbaniczky S., Östlin H., and Malmqvist M. 1991. Real-time biospecific interaction analysis using surface plasmon resonance and a sensor chip technology. *BioTechniques* 11: 620–627.

Kallweit U., Börnsen K.O., Kresbach G.M., and Widmer H.M. 1996. Matrix compatible buffers for analysis of proteins with matrix-assisted laser desorption/ionization mass spectrometry. *Rapid Commun. Mass Spectrom.* 10: 845–849.

Kretschmann E. 1971. Die Bestimmung optischer Konstanten von Metallen durch Anregung von Oberflächenplasmaschwingungen. *Z. Physik* 241: 313–324.

Kussmann M. and Roepstorff P. 2000. Sample preparation techniques for peptides and proteins analyzed by MALDI-MS. *Methods Mol. Biol.* 146: 405–424.

Lackmann M., Bucci T., Mann R.J., Kravets L.A., Viney E., Smith F., Moritz R.L., Carter W., Simpson R.J., Nicola N.A., Mackwell K., Nice E.C., Wilks A.F., and Boyd A.W. 1996. Purification of a ligand for the EPH-like receptor HEK using a biosensor-based affinity detection approach. *Proc. Natl. Acad. Sci.* 93: 2523–2527.

Markgren P.O., Hamalainen M., and Danielson U.H. 1998. Screening of compounds interacting with HIV-1 proteinase using optical biosensor technology. *Anal. Biochem.* 265: 340–350.

Nagata K. and Handa H., eds. 2000. *Real-time analysis of biomolecular interactions: Applications of BIACORE.* Springer-Verlag, Tokyo, Japan.

Natsume T., Nakayama H., and Isobe T. 2001. BIA-MS-MS: Biomolecular interaction analysis for functional proteomics. *Trends Biotechnol.* 19 s28–s33.

Natsume T., Nakayama H., Jansson Ö., Isobe T., Takio K., and Mikoshiba K. 2000. Combination of biomolecular interaction analysis and mass spectrometric amino acid sequencing. *Anal. Chem.* 72: 4193–4198.

Natsume T., Taoka M., Manki H., Kume S., Isobe T., and Mikoshiba K. 2002. Rapid analysis of protein interactions: On-chip micropurification of recombinant protein expressed in *Escherichia coli*. *Proteomics* 2: 1247–1453.

Nelson R.W. and Krone J.R. 1999. Advances in surface plasmon resonance biomolecular interaction analysis mass spectrometry (BIA/MS). *J. Mol. Recog.* 12: 77–93.

Sakano S., Serizawa R., Inada T., Iwama A., Itoh A., Kato C., Shimizu Y., Shinkai F., Shimizu R., Kondo S., Ohno M., and Suda T. 1996. Characterization of a ligand for receptor protein-tyrosine kinase HTK expressed in immature hematopoietic cells. *Oncogene* 13: 813–822.

Seok Y.J., Sondej M., Badawi P., Lewis M.S., Briggs M.C., Jaffe H., and Peterkofsky A. 1997. High affinity binding and allosteric regulation of *Escherichia coli* glycogen phosphorylase by the histidine phosphocarrier protein, HPr. *J. Biol. Chem.* 272: 26511–26521.

Simpson R.J. 2003. *Proteins and proteomics: A laboratory manual.* Cold Spring Harbor Laboratory Press, Cold Spring Harbor, New York.

Sönksen C.P., Nordhoff E., Jansson Ö., Malmqvist M., and Roepstorff P. 1998. Combining MALDI mass spectrometry and biomolecular interaction analysis using a biomolecular interaction analysis instrument. *Anal. Chem.* 70: 2731–2736.

Stenberg E., Persson B., Roos H., and Urbaniczky C. 1991. Quantitative determination of surface concentration of protein with surface plasmon resonance by using radiolabeled proteins. *J. Colloid Interface Sci.* 143: 513–526.

Ward L.D. and Winzor D.J. 2000. Relative merits of optical biosensors based on flow-cell and cuvette designs. *Anal. Biochem.* 285: 179–193.

Williams C. 2000. Biotechnology match making: Screening orphan ligands and receptors. *Curr. Opin. Biotechnol.* 11: 42–46.

Williams C. and Addona T.A. 2000. The integration of SPR biosensors with mass spectrometery: Possible applications for proteome analysis. *Trends Biotechnol.* 18: 45–48.

Wilm M. and Mann M. 1996. Analytical properties of the nanoelectrospray ion source. *Anal. Chem.* 68: 1–8.

Winzor D.J. 2003. Surface plasmon resonance as a probe of protein isomerization. *Anal. Biochem.* 318: 1–12.